

NASA/CR—2003-212100



Micro-Optical Distributed Sensors for Aero Propulsion Applications

S. Arnold and V. Otugen
Polytechnic University, Brooklyn, New York

January 2003

The NASA STI Program Office . . . in Profile

Since its founding, NASA has been dedicated to the advancement of aeronautics and space science. The NASA Scientific and Technical Information (STI) Program Office plays a key part in helping NASA maintain this important role.

The NASA STI Program Office is operated by Langley Research Center, the Lead Center for NASA's scientific and technical information. The NASA STI Program Office provides access to the NASA STI Database, the largest collection of aeronautical and space science STI in the world. The Program Office is also NASA's institutional mechanism for disseminating the results of its research and development activities. These results are published by NASA in the NASA STI Report Series, which includes the following report types:

- **TECHNICAL PUBLICATION.** Reports of completed research or a major significant phase of research that present the results of NASA programs and include extensive data or theoretical analysis. Includes compilations of significant scientific and technical data and information deemed to be of continuing reference value. NASA's counterpart of peer-reviewed formal professional papers but has less stringent limitations on manuscript length and extent of graphic presentations.
- **TECHNICAL MEMORANDUM.** Scientific and technical findings that are preliminary or of specialized interest, e.g., quick release reports, working papers, and bibliographies that contain minimal annotation. Does not contain extensive analysis.
- **CONTRACTOR REPORT.** Scientific and technical findings by NASA-sponsored contractors and grantees.

- **CONFERENCE PUBLICATION.** Collected papers from scientific and technical conferences, symposia, seminars, or other meetings sponsored or cosponsored by NASA.
- **SPECIAL PUBLICATION.** Scientific, technical, or historical information from NASA programs, projects, and missions, often concerned with subjects having substantial public interest.
- **TECHNICAL TRANSLATION.** English-language translations of foreign scientific and technical material pertinent to NASA's mission.

Specialized services that complement the STI Program Office's diverse offerings include creating custom thesauri, building customized databases, organizing and publishing research results . . . even providing videos.

For more information about the NASA STI Program Office, see the following:

- Access the NASA STI Program Home Page at <http://www.sti.nasa.gov>
- E-mail your question via the Internet to help@sti.nasa.gov
- Fax your question to the NASA Access Help Desk at 301-621-0134
- Telephone the NASA Access Help Desk at 301-621-0390
- Write to:
NASA Access Help Desk
NASA Center for Aerospace Information
7121 Standard Drive
Hanover, MD 21076

NASA/CR—2003-212100



Micro-Optical Distributed Sensors for Aero Propulsion Applications

S. Arnold and V. Otugen
Polytechnic University, Brooklyn, New York

Prepared under Grant NAG3-2679

National Aeronautics and
Space Administration

Glenn Research Center

January 2003

The Propulsion and Power Program at
NASA Glenn Research Center sponsored this work.

Available from

NASA Center for Aerospace Information
7121 Standard Drive
Hanover, MD 21076

National Technical Information Service
5285 Port Royal Road
Springfield, VA 22100

Available electronically at <http://gltrs.grc.nasa.gov>

Micro-Optical Distributed Sensors for Aero Propulsion Applications

S. Arnold and V. Otugen
Polytechnic University
Brooklyn, New York 11201

Summary

The objective of this research is to develop micro-opto-mechanical system (MOMS)-based sensors for time- and space-resolved measurements of flow properties in aerodynamics applications. The measurement technique we propose uses optical resonances in dielectric microspheres that can be excited by radiation tunneling from optical fibers. It exploits the tunneling-induced and morphology-dependent shifts in the resonant frequencies. The shift in the resonant frequency is dependent on the size, shape and index of refraction of the micro-sphere. A physical change in the environment surrounding a micro-bead can change one or more of these properties of the sphere thereby causing a shift in frequency of resonance. The change of the resonance frequency can be detected with high resolution by scanning a frequency-tunable laser that is coupled into the fiber and observing the transmission spectrum at the output of the fiber. It is expected that, in the future, the measurement concept will lead to a system of distributed micro-sensors providing spatial data resolved in time and space. The present project focuses on the development and demonstration of temperature sensors using the morphology-dependent optical resonances although in the latter part of the work, we will also develop a pressure sensor. During the period covered in this report, the optical and electronic equipment necessary for the experimental work was assembled and the experimental setup was designed for the single sensor temperature measurements. Software was developed for real-time tracking of the optical resonance shifts. Some preliminary experiments were also carried out to detect temperature using a single bead in a water bath.

Introduction

We are interested in using resonances or, the so-called Whispering Gallery Modes (WGM), of a microsphere as a sensor for properties of the local environment. The resonances are of extremely high Q and are caused by the entrapment of photons due to total internal reflection. The light orbits the microsphere as illustrated in Fig. 1 (i.e. wave point of view). Each orbit has a constant number of wavelengths l , similar to orbits within a Bohr atom. Consequently the circumference will be equal to a whole number of internal wavelengths,

$$2\pi a \approx l \lambda/n \quad (1)$$

where n is the refractive index of the sphere and a is its radius. As a consequence of Eq. (1), any change in the size of the particle or its refractive index leads to a certain resonance shift. In the case of temperature, the sensitivity can be extremely large. In quartz microspheres of sub-millimeter size Q values of 10^{10} have been reported. The thermal expansion coefficient of quartz is $\sim 10^{-6} \text{ K}^{-1}$, which translates into a sensitivity for temperature change of 10^{-5} K . Considering that fused silica has a particularly small thermal expansion coefficient, the extreme sensitivity to temperature is surprising. It is clearly a consequence of the large quality factor associated with the resonances. To drive a WGM, we utilize a particular discovery made at the Polytechnic.

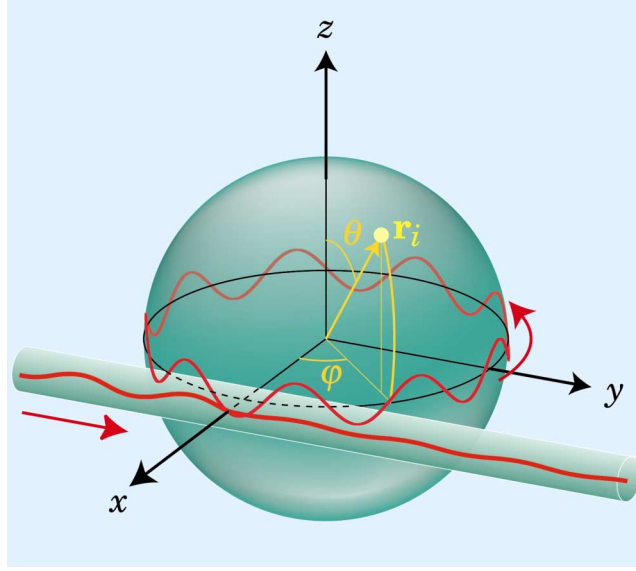


Figure 1. Stimulation of a Microsphere Resonance by a naked optical fiber.

A fiber etched to its core with its evanescent field overlapping the evanescent field of the spherical mode can stimulate a mode (as depicted in Fig. 1). Therefore, it is possible to couple light into an optical microbead from a bare fiber that is touching it if the frequency of the light traveling through the fiber matches one of the resonances of the bead. Thus, one can interrogate the resonances of the bead by scanning a tunable laser that is coupled into the fiber. The location of the resonances can be monitored by observing the dips in the transmitted light through the fiber by means of a photo detector.

Theory

The electrical field within a dielectric particle satisfies the vector Helmholtz equation of the form,^{1,2}

$$\nabla^2 \vec{E} + k^2 \vec{E} = 0 \quad (2)$$

where $k = nk_0$ is the wave vector, where k_0 is the vacuum wave vector and n is the refractive index. In the spherical coordinates, the equation becomes

$$\frac{\partial^2}{r \partial r^2} r \vec{E} - \frac{\hat{L}^2}{r^2} \vec{E} + k^2 \vec{E} = 0 \quad (3)$$

where \hat{L} is the angular momentum operator $\hat{L} = i\vec{r} \times \nabla$. We note the commutation relationship between \hat{L} and \hat{L}^2 . The solution of the field therefore can be written as

$$\vec{E} = \frac{\hat{L} \psi}{r} \quad (4)$$

where ψ is a scalar function, so that one only needs to solve following one-dimensional equation.

$$\frac{\partial^2 \psi}{\partial r^2} - \frac{\hat{L}^2}{r^2} \psi + n^2 k_0^2 \psi = 0 \quad (5)$$

For a sphere, the refractive index can be described as:

$$\begin{cases} n = n & r \leq a \\ n = n_s & r > a \end{cases} \quad (6)$$

where a is the radius of the spherical bead, n is the absolute refractive index of the bead material, n_s is the refractive index of surrounding material. For example, the approximate refraction index for silica, air, and water are 1.53, 1, and 1.33, respectively.

The solutions of Eq. (5) with boundary conditions (6) are the Ricatti-Bessel functions. These functions correspond to the electrical mode inside the sphere. The resonance frequencies are related to the complex eigenvalues $\{k_o\}$. The complex number indicates the light leakage from the sphere. For a sphere with a radius around several hundred microns, a geometric picture of the internal reflection can lead to an approximation resonance solution³ given earlier by Eq. (1) for wavelength

$$l\lambda = 2\pi na$$

where l is an integral number and is the same as the quantum number of angular momentum, \hat{L}^2 .

The leaking rate is very small for an isolated sphere. However, the tunneling loss increases significantly when the sphere is put very close to a fiber. Conversely, light in fiber can also tunnel into the sphere. The tunneling effect becomes much stronger when the light matches the electromagnetic mode of the sphere. Therefore we expect to see resonant absorption by the sphere at the wavelengths given by Eq. (1).

When a temperature change induces a change in the refractive index and the radius of the bead, the resonant wavelength also changes. From Eq. (1)

$$\frac{\Delta\lambda}{\lambda} = \frac{\Delta(n_0 a)}{n_0 a} = \frac{\Delta a}{a} + \frac{\Delta n_0}{n_0} = \alpha\Delta T + \beta\Delta T = (\alpha + \beta)\Delta T \quad (7)$$

$$\Delta T = \frac{1}{\alpha + \beta} \frac{\Delta\lambda}{\lambda} \quad (8)$$

where, α is the thermal expansion coefficient, β is the thermal coefficient of refractive index, and T is temperature of the bead. The thermal expansion coefficient for silica is $\alpha = 5.5E-7 \text{ } ^\circ\text{C}^{-1}$ while the thermal coefficient of refractive index is $\beta = 8.53 E-6 \text{ } ^\circ\text{C}^{-1}$. Most other glass materials have smaller thermal coefficient of refractive index than silica.

We note that if the micro bead shape is not spherical, its resonance wavelengths cannot be described by the simple relation in Eq. (1). For a bead with a quadrupole shape⁴ it is defined as

$$\begin{cases} n = n & r \leq a[1 + e\sqrt{4\pi}Y_{2,0}(\theta, \varphi)] \\ n = n_s & r > a[1 + e\sqrt{4\pi}Y_{2,0}(\theta, \varphi)] \end{cases} \quad (9)$$

where, e is the small deviation coefficient, $e = \frac{2}{3\sqrt{5}} \frac{r_{\max} - r_{\min}}{a}$. The new resonant position deviates from the corresponding sphere resonant position by

$$\lambda_m = \lambda_0 \left[1 + \frac{e}{3} \left(1 - \frac{3m^2}{l(l+1)} \right) \right] \quad (10)$$

where $m = -l, \dots, l$, and λ_0 is the quantum number l -related resonant wavelength of sphere with radius a , determined by Eq. (1).

Progress

During the initial period of February 1 to September 30, 2002, an experimental set up was designed and manufactured and software was developed for automatic data acquisition and processing to track optical resonance frequency shifts in micro-beads in response to changes their surrounding. A post-doctoral fellow, Dr. Jason Guan has come aboard and begun to assemble a highly sensitive precision spectrometer with which to measure the physical properties of the microsphere resonances under temperature perturbations.

Experimental Setup

We designed an experiment to measure the resonant frequency shift and infer the temperature from that shift. A schematic of the experimental setup is shown in Fig. 2. The set up consists of a laser source, operating around 1306 nm wavelength and associated optical, electronic and mechanical elements including mounts, controller, etc. The laser controller can be driven by an external voltage signal. The laser beam is coupled into a single mode fiber (Corning SMF-28 single mode fiber) using a Newport single mode coupler F-1015LD. Light in the fiber travels only inside the core. The core diameter of SMF-28 single mode fiber is 8 microns. The details of the test section is shown in Fig. 3. In the test section, a certain length of the fiber is stripped of its cladding and the core fiber is etched to a diameter of about 4 to 5 μm . A silica bead is made by heating fiber in a micro-torch. The diameter of the spheroid-shaped bead ranges from 150 to 400 μm . The bead is placed such that it touches the bare fiber around the bead's maximum diameter. A photograph of this sensor arrangement is shown in Fig. 4. The optical sensor is placed in a small water bath along with a thermistor as shown in Fig. 3. The Thermometrics micro-thermistor MC65F103A is used to monitor the temperature change. We use operational amplifier to make a constant current source. The voltage between two legs of the thermistor is proportional to the resistance, which is a strong function of temperature.

An InGaAs photodiode detector measures the transmission laser light intensity at the end of the fiber. The voltage output of the photodiode is fed into a 16-bit analog-to-digital converter (National Instruments PCI 6036E DAQ card) that is connected to a personal computer that controls the data acquisition and performs the real time analysis. We developed a Labview-based software to acquire and analyze the data.

A function generator (HP 3325A) provides input to the laser diode controller and the DAQ card during the experiment. It provides a ramp function to the laser diode controller and square wave signal to trigger input of the DAQ card in order to synchronize the data acquisition with the scanning of the laser. The ramp signal allows for a linear increase of the laser current with time. A transmission spectrum is obtained for each ramp cycle. The Labview software is designed to follow the absorption resonance, which indicates the sphere property and thus contains the environmental change information. In our preliminary measurements, the sensor is immersed in water in order to avoid rapid changes in temperature of the environment of the bead sensor.

The thermal relaxation time of the small water bath is in the order of several seconds whereas this time is in the order of a millisecond for the sensor bead itself. In the initial development of the measurement technique, we would like to first test the system and the associated software in a slow time-varying environment. In the future, we will progressively increase the frequency of temperature variations and track the resonances in order to make fast and accurate temperature measurements.

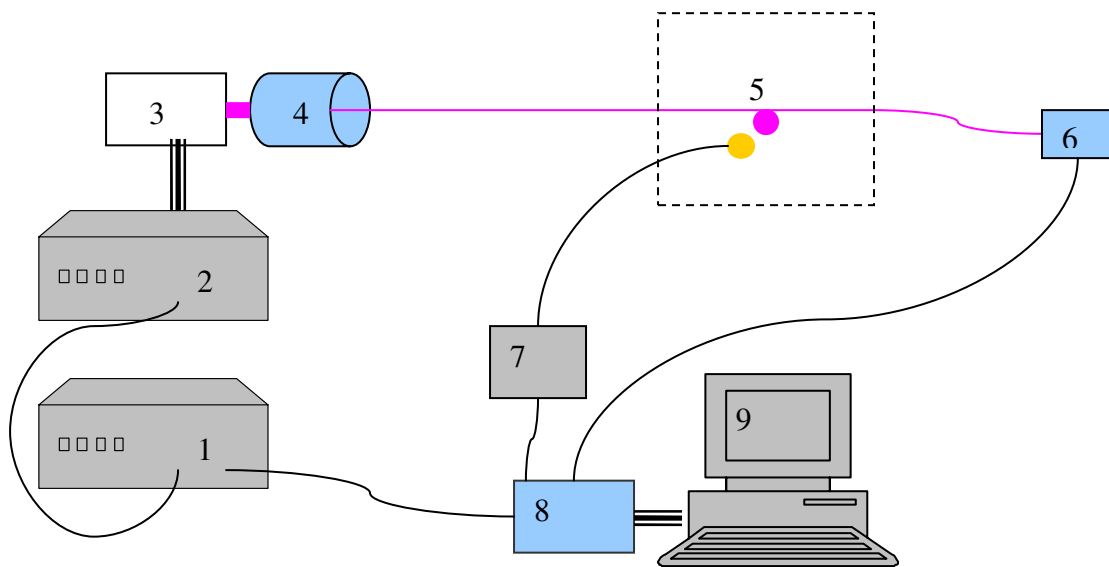


Figure 2. Experimental setup: 1-Function generator; 2-Laser diode controller; 3-DFB laser diode; 4-Single mode fiber coupler; 5-Test section; 6-Photodiode; 7-Resistance-Voltage converter; 8-National Instrument DAQ card; 9-Personal computer.

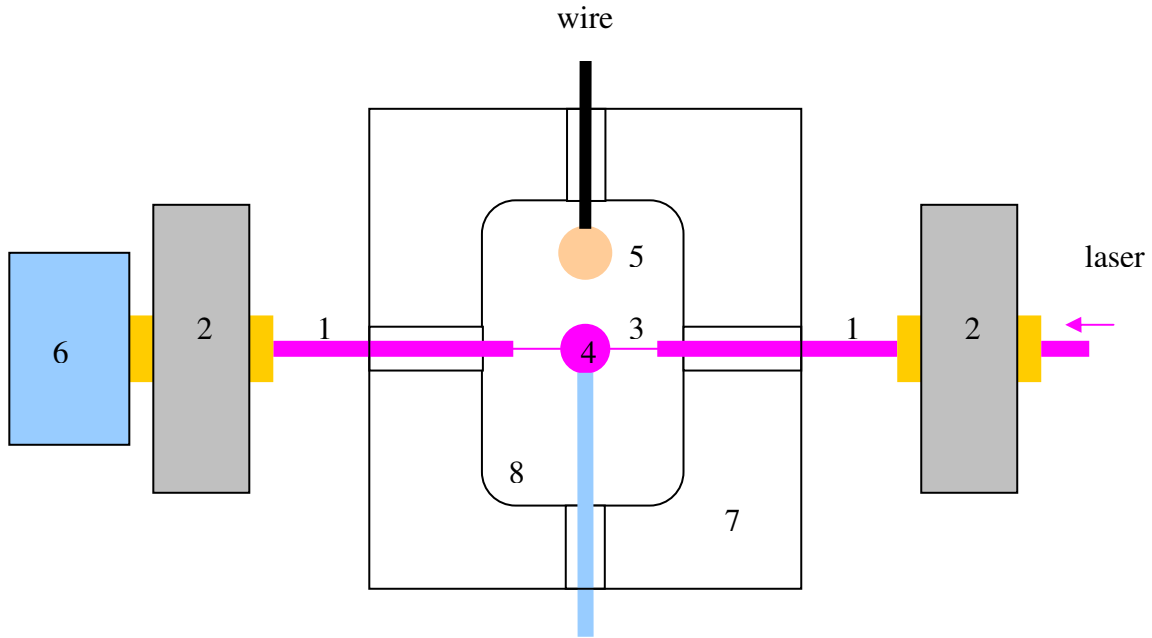


Figure 3. Top view of test section; 1-Fiber; 2-Fiber holder; 3-Etched section of fiber; 4-Silica bead; 5-Thermistor; 6-InGaAs Photodiode; 7-Glass cell; 8-Water bath.

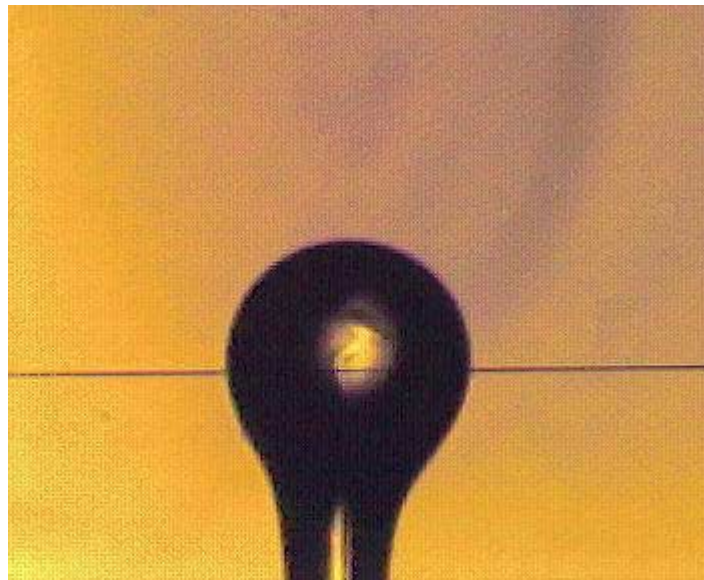


Figure 4. Photo of MOMS sensor: Fiber diameter $\sim 5 \mu\text{m}$ and sphere diameter $\sim 350 \mu\text{m}$.

Choice of Laser Source

It is conventional in high-resolution spectroscopy to use a semiconductor laser having an electro-mechanically tuned external cavity. Since we wanted our system to be both miniature and fast, we substituted this by an electronically-tuned Distributed Feedback Laser (DFB). This choice not only allows for much more rapid tuning, but also anticipates an integrated optics solution. DFB lasers are of a single heterojunction type with a grating imprinted within their structure. This constrains the laser to operate at a single frequency with a linewidth of ~ 30 MHz. The frequency of the laser can be rapidly modulated ($> \text{MHz}$) by perturbing electronic state populations using the drive current. We use an ILX Lightwave LDC-3714B laser diode controller and Mitsubishi ML725B11F DFB laser diode in our setup. The laser controller can be driven by an external voltage signal. A Newport F-1015LD single-mode fiber coupler allows us to focus energy into a single-mode fiber.

The laser operates around 1306 nm wavelength. This is a wavelength widely used in the telecommunications industry. Thus we can find suitable and economic laser diode and associated optical elements fairly easily.

Microsphere and Eroded Fiber Fabrication

We use bare single mode fiber (Corning SMF-28) as our sphere material. The microsphere is formed by using a micro-torch to melt the fiber end. As a result, a spherical droplet forms at the end of the fiber. The sphere size is controlled from the amount of melted glass (i.e. heating time). A typical sphere is shown above in Fig. 4. In the figure, the thin line is the image of the $4\mu\text{m}$ diameter etched fiber that is used to excite WGM's of the sphere. The bare fiber is fabricated through chemical etching with concentrated hydrofluoric acid over a 12 mm length. The fiber is etched into the core. Although the un-etched core is $8\mu\text{m}$ in diameter, the diameter of the etched core is ~ 4 to $5\mu\text{m}$.

Alternate Measurement Cell Design

The preliminary measurements that will be described later in the report were carried out using the test cell arrangement shown in Fig. 3. However, an alternate cell is also developed and is currently being tested in connection with measuring the effect of temperature, stress and other environmental influences on the microsphere resonances. Figure 5 shows this cell design.

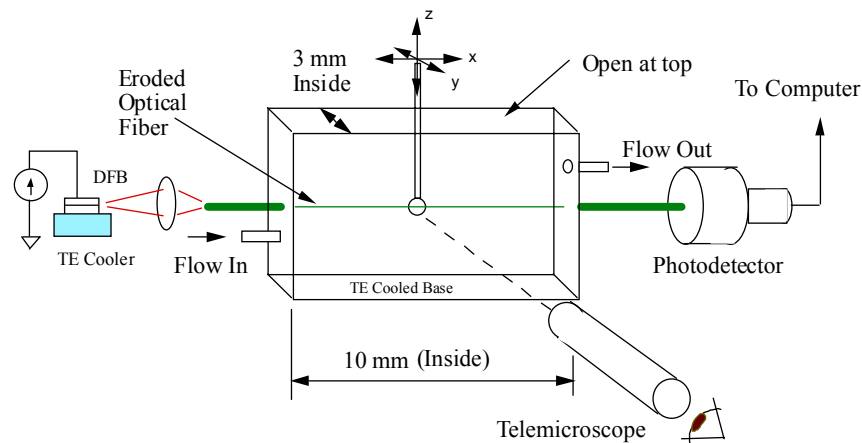


Figure 5. Cell for controlling the environment of the microsphere.

In this design, the enclosure entraps air (rather than water) with inlet and outlet ports. The cell is cooled at the bottom. We expect that the temperature of the air will be tightly controlled with this arrangement.

Frequency Tracking Software

The 16-bit DAQ card is installed in the personal computer as the interface for analog/digital converting. An external square signal is provided to the DAQ card for triggering. The voltage signal from photodiode is sampled by the DAQ card. The voltage signal from the thermistor is also sampled by the DAQ card. The square signal from the function generator (synchronized with the ramp signal provided to the laser controller) is also fed to the DAQ card as trigger.

We chose to use National Instruments' Labview as our measurement platform. A Labview program is designed to acquire the data and perform the analysis. The program front panel is shown in Fig. 6. The function generator generates a ramp signal at a specified magnitude with a scan frequency of 30 Hz. This scan frequency, current offset and modulation magnitude are provided to the Labview program to calculate the scan range. The DAQ card samples 500 points in each scan (or ramp cycle). Sampling starts whenever an external trigger signal is received. Therefore, the actual data-record rate is smaller than the scan rate. We have about 15 Hz data record rate when scan rate is at 30 Hz and sampling rate is 500 points per scan. A real time spectral diagram of light intensity against laser current is plotted in the center of the display window (Fig. 6). The Labview program also gives the option to display all results in light

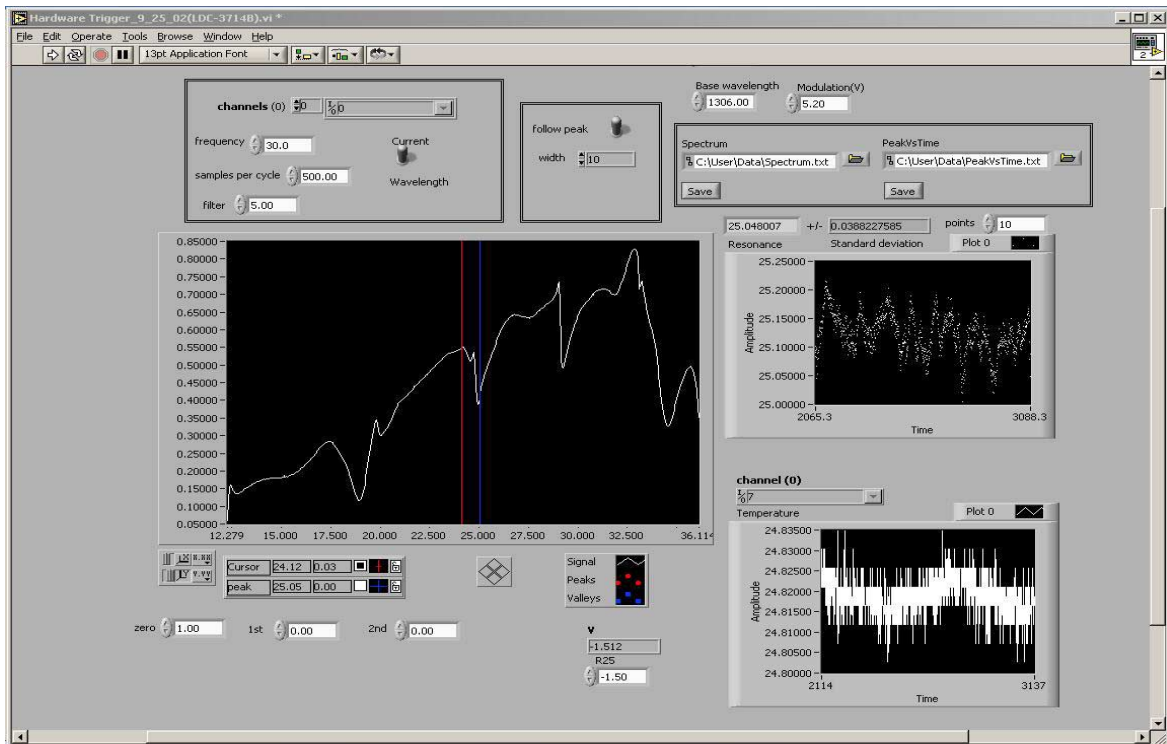


Figure 6. Labview program front panel.

wavelength since the laser wavelength is uniquely determined by the driving laser current. There are several resonant absorptions in our scan range, each of which corresponds to an electromagnetic resonant mode of the bead. We use an algorithm that fits a quadratic polynomial to sequential groups of data points representing a dip (for example 10 points in Fig. 6) to determine the resonance positions in the spectrum. The software locks into a simple resonance by finding the minimum shift between two consecutive scans. The scan is fast enough so that the resonance shift between two consecutive scans does not exceed the free spectral range (overtaking of one resonance dip the next one by a large frequency shift). Therefore, in this mode, as long as the temperature driven resonance shifts are slower than the data acquisition and analysis speed, resonance shifts larger than the free spectral range can be easily measured.

A diagram of resonance positions versus time is plotted at the right of the spectral diagram. The program also samples the resistance of thermistor after each current scan. The temperature is calculated from the resistance. Temperatures versus time are plotted in the low right corner. The spectrum, the resonance and the temperature can be saved at any time.

Calibration of the Laser Wavelength

We calibrate the DFB laser wavelength by using Burleigh Instruments wavemeter WA-1150. Figure 7 shows the relation between the wavelength of the DFB laser and the driving current. The black symbols are the measured wavelength at each driving current. The solid red line is a fit function using a second order polynomial as follows

$$\lambda = 1306.30205 + 0.00465 I + 0.0000566 I^2 \quad (11)$$

where, the wavelength, λ , is in nanometers and the current, I , is in mA. The accuracy of wavelength by fitting is better than 0.001 nm, which for silica sphere represents 0.08 °C error in temperature measurement.

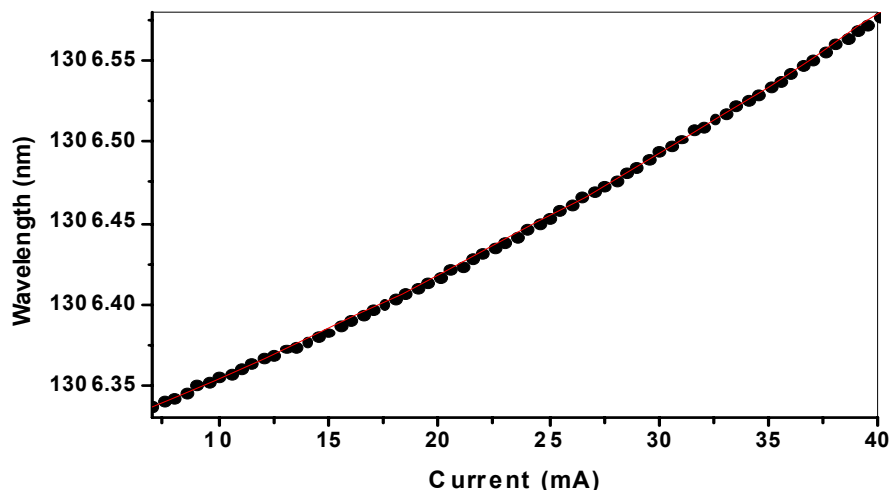


Figure 7. Laser wavelength versus current.

Results

We carried out measurements in water using the test section of Fig. 3. The glass cavity filled with water. The thermistor is placed near the sphere to monitor the temperature of water as shown in Fig 3. The bead, the fiber, and the thermistor are all immerse in the water. The bead and fiber touch each other as shown. The function generator generates ramp signal at 30 Hz repetition rate. 500 points of the photodiode are sampled at each ramp cycle. Sampling starts whenever an external trigger signal is received. As discussed before, the actual measurement rate is 15 Hz.

A typical scan spectrum is shown in Fig. 8. There are usually several resonances in one spectrum. The Labview program locks the cursor to one resonance position as indicated by the arrow. The resonance position is related to the bead size, shape and index of refraction. A slight change in bead temperature can induce significant change in the position of the particular resonance. Thus, when we measure the shift in the resonance position, we can infer the change in temperature provided that there are no additional changes in the environmental conditions other than temperature. During the experiment, we heat the air around the test section with a heat gun thereby causing a change in the temperature of water surrounding the sensor bead. We independently measure the temperature of the water using the thermistor during the experiments. The results of a typical experiment are shown in Fig. 9. Here, the temperature measured by the optical sensor is compared to that form the thermistor. The optical measurement is made by tracking the shift of the resonance dip identified in Fig. 8. The shift is converted to temperature using Eq. (8).

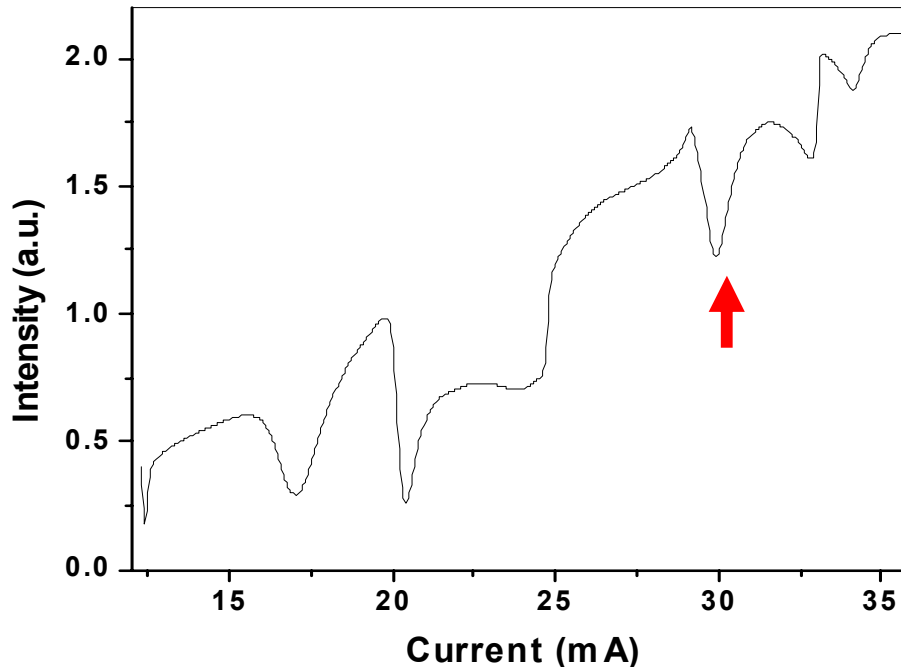


Figure 8. Transmission spectrum in a typical run.

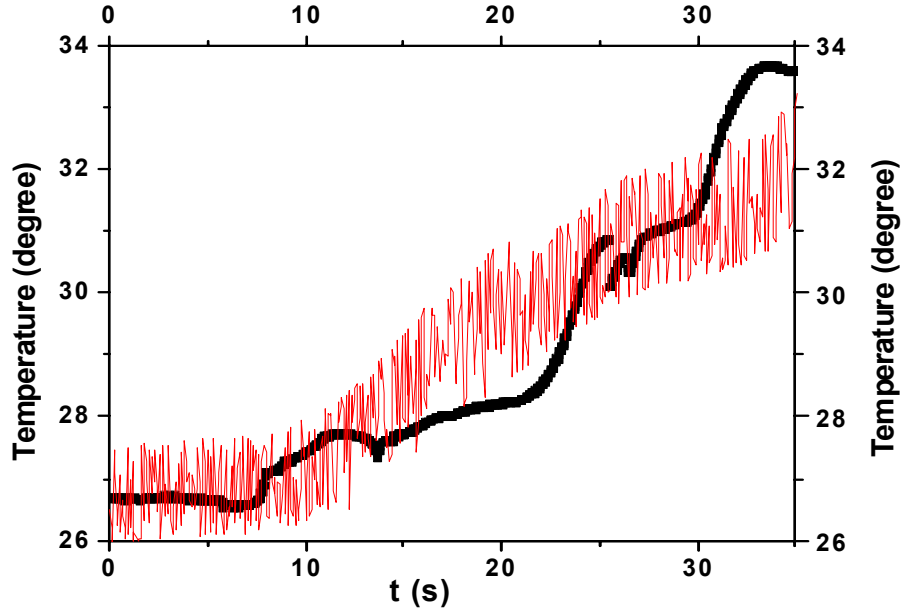


Figure 9. Measured temperature against time: Black dot by bead and red line by thermistor.

Discussion

The temperature increases by a total amount of ~ 5.5 °C during heating according to the thermistor measurement. The resonance shifts by a total amount of ~ 10 mA at the end of the heating. The corresponding temperature change calculated from Eq. (8) is about 6.7 °C. Figure 9 shows that the two temperatures match each other reasonably well although there are slight mismatches between them as time progresses. However, we note that there is no significant relative bias between the two types of measurements. The mismatch is believed to be primary due to non-homogeneous heating of the water in the enclosure by the heat gun, particularly considering that the thermal relaxation time of the water in the enclosure is several tens of seconds. It is noted that the contribution to resonant shift comes primary from change in refractive index for silica material (rather than the diameter change of the bead) since silica has very small thermal expansion coefficient. It turns out that silica is the best material to sense the temperature due to large thermal coefficient of refractive index.

We call the “free spectral range” (FSR) the wavelength jump between two consecutive resonances. Typically, FSR determines the upper bound of the dynamic range of the measurement unless the measurement is fast enough to lock onto a specific resonance and track it past a the FSR. An approximate calculation of the free spectral range can be accomplished using Eq. (10) for the quadrupole shape particle as follows

$$\frac{\lambda_m - \lambda_{m-1}}{\lambda_0} = \frac{(2m - 1)e}{l(l + 1)} \cong (2m - 1)e \frac{\lambda_0^2}{4\pi^2 a^2} \quad (12)$$

We can also obtain the FSR from the measured spectrum. For example, in Fig. 8 the two adjacent resonances are separated by about 3 mA, which corresponds to 0.024 nm in wavelength and about 2 °C of temperature change for the silica bead. To ensure that the software successfully

locks on one resonance and tracks its shift, the measurement rate should be high enough so that resonance shift is less than half of the free spectrum or (1 °C in the present setup). At 15 Hz measurement rate, we can successfully measure temperature change rates up to about 10 °C/s. Again, these numbers are for the present setup and software which is only a preliminary effort. We expect to improve these numbers significantly in the near future by both hardware and software. Also, we will carry out temperature measurements with the improved test section (cell) that has provides a much more uniform temperature distribution within it.

References

1. J.D. Jackson, "Classical Electrodynamics," John Wiley & Sons, Inc, 3rd edition, p. 380 (1998).
2. B.E. Little, J.P. Laine, and H.A. Haus, J. Lightwave Technology, vol. 17, no. 4, p. 704 (1999).
3. R.K. Chang and A.J. Campilla, "Optical processes in microcavities," World Scientific Publishing Co. Pte. Ltd., p. 10 (1996).
4. H.M. Lai, P.T. Leung, and K. Young, Physical Review A, 41, no.9, p. 5187 (1990).

REPORT DOCUMENTATION PAGE			<i>Form Approved</i> <i>OMB No. 0704-0188</i>	
Public reporting burden for this collection of information is estimated to average 1 hour per response, including the time for reviewing instructions, searching existing data sources, gathering and maintaining the data needed, and completing and reviewing the collection of information. Send comments regarding this burden estimate or any other aspect of this collection of information, including suggestions for reducing this burden, to Washington Headquarters Services, Directorate for Information Operations and Reports, 1215 Jefferson Davis Highway, Suite 1204, Arlington, VA 22202-4302, and to the Office of Management and Budget, Paperwork Reduction Project (0704-0188), Washington, DC 20503.				
1. AGENCY USE ONLY (Leave blank)		2. REPORT DATE January 2003	3. REPORT TYPE AND DATES COVERED Final Contractor Report	
4. TITLE AND SUBTITLE Micro-Optical Distributed Sensors for Aero Propulsion Applications			5. FUNDING NUMBERS WBS-22-708-87-23 NAG3-2679	
6. AUTHOR(S) S. Arnold and V. Otugen				
7. PERFORMING ORGANIZATION NAME(S) AND ADDRESS(ES) Polytechnic University Six Metro Tech Center Brooklyn, New York 11201			8. PERFORMING ORGANIZATION REPORT NUMBER E-13753	
9. SPONSORING/MONITORING AGENCY NAME(S) AND ADDRESS(ES) National Aeronautics and Space Administration Washington, DC 20546-0001			10. SPONSORING/MONITORING AGENCY REPORT NUMBER NASA CR-2003-212100	
11. SUPPLEMENTARY NOTES Project Manager, Richard G. Seasholtz, Instrumentation and Controls Division, NASA Glenn Research Center, organization code 5520, 216-433-3754.				
12a. DISTRIBUTION/AVAILABILITY STATEMENT Unclassified - Unlimited Subject Category: 35 Available electronically at http://gltrs.grc.nasa.gov This publication is available from the NASA Center for AeroSpace Information, 301-621-0390.			12b. DISTRIBUTION CODE	
13. ABSTRACT (Maximum 200 words) The objective of this research is to develop micro-opto-mechanical system (MOMS)-based sensors for time- and space-resolved measurements of flow properties in aerodynamics applications. The measurement technique we propose uses optical resonances in dielectric micro-spheres that can be excited by radiation tunneling from optical fibers. It exploits the tunneling-induced and morphology-dependent shifts in the resonant frequencies. The shift in the resonant frequency is dependent on the size, shape, and index of refraction of the micro-sphere. A physical change in the environment surrounding a micro-bead can change one or more of these properties of the sphere thereby causing a shift in frequency of resonance. The change of the resonance frequency can be detected with high resolution by scanning a frequency-tunable laser that is coupled into the fiber and observing the transmission spectrum at the output of the fiber. It is expected that, in the future, the measurement concept will lead to a system of distributed micro-sensors providing spatial data resolved in time and space. The present project focuses on the development and demonstration of temperature sensors using the morphology-dependent optical resonances although in the latter part of the work, we will also develop a pressure sensor. During the period covered in this report, the optical and electronic equipment necessary for the experimental work was assembled and the experimental setup was designed for the single sensor temperature measurements. Software was developed for real-time tracking of the optical resonance shifts. Some preliminary experiments were also carried out to detect temperature using a single bead in a water bath.				
14. SUBJECT TERMS Temperature measurements; MOMS sensors			15. NUMBER OF PAGES 18	
			16. PRICE CODE	
17. SECURITY CLASSIFICATION OF REPORT Unclassified	18. SECURITY CLASSIFICATION OF THIS PAGE Unclassified	19. SECURITY CLASSIFICATION OF ABSTRACT Unclassified	20. LIMITATION OF ABSTRACT	

